

Prediction of Brain MR Scans in Longitudinal Tumor Follow-Up Studies

Lior Weizman¹, Liat Ben-Sira², Leo Joskowicz¹, Orna Aizenstein²,
Ben Shofty², Shlomi Constantini², and Dafna Ben-Bashat²

¹ School of Eng. and Computer Science, Hebrew University of Jerusalem, Israel

² Sourasky Medical Center, Tel-Aviv, Israel

`lweizm45@cs.huji.ac.il`

Abstract. We present a new method for the estimation of the next brain MR scan in a longitudinal tumor follow-up study. Our method effectively incorporates information of the past scans in the time series to predict the future scan of the patient. Its advantages are that it requires no user intervention and does not assume any particular tumor growth model. Instead, the patient-specific tumor growth parameters are estimated individually from the past patient scans. To validate our method, we conducted an experimental study on four patients with Optic Path Gliomas (OPGs) and four patients with glioblastomas multiforma (GBM), each scanned at five time points. The tumor volumes in the predicted and actual future scans, both segmented by an expert radiologist, yield a mean volume overlap difference of 13.65% for the OPG patients, and 34.23% for the GBM patients.

1 Introduction

Brain tumor detection, characterization, and follow-up using CT and MR images is the current standard of care in neuroradiology. The decision making process takes into consideration previous scans of the patient, and aims at detecting visual clues (markers) that indicate tumor progression, regression, or stable disease. However, the estimation of these trends is a difficult task due to tumor inhomogeneity, inter-scans variations, and the lack of practical tools to estimate the tumor volume consistently and reliably.

The prediction of tumor growth is a challenging task. The natural growth of tumor cells does not always adhere to a specific growth model. Additionally, changes in the tumor growth resulting from different therapies are still largely unknown and unexplored, and therefore are not amenable to analytic modeling. Thus, in practice, prediction methods aim at providing a coarse estimate of the future involvement areas of the tumor, rather than predicting the exact future spatial extent and volume of the tumor.

The current literature on tumor progression prediction consists of two main approaches. The first one relies on tumor growth models. The models describe the evolution of the tumor cells over time at a microscopic and/or macroscopic level. Hogeia et al. [1] propose a model that couples glioma growth with the

subsequent deformation of the brain tissue. Clatz et al. [2] describe a model that simulates the volumetric growth of glioblastomas multiforma (GBM). The model is derived from two subsequent MRI scans of a patient acquired at six months intervals. While promising, the model parameters are independently estimated from a single scan without incorporating the other parameters related to the natural history of the patient.

The second approach to tumor progression prediction assumes a model derived from the tumor growth pattern from the patient scans. For example, [3] shows how to predict response to therapy based on the derived apparent diffusion coefficients (ADCs) values computed from diffusion-weighted magnetic resonance imaging (DWMRI). Loncaster et al. [4] use measured volumes and signal intensities in T1 MRI scans to predict radiotherapy outcome. Note that these works focus on the prediction of response to a specific treatment on a predefined area of interest rather than aim at predicting an entire future scan.

We present a new algorithm to compute the predicted MRI scan of the entire brain based on imaging markers trends derived from the past scans of the patient in a longitudinal study (the second approach above). The method computes the optical flow of the voxels over time, and uses past motion vectors to predict a new deformable field, which is then used to estimate the next scan in the time series. Two key advantages of our method are that it takes into account multiple past scans of the patient and that it can be applied to a variety of brain tumors types since the tumor growth model prediction parameters are estimated from the scans of the patient itself instead of from tumor-specific growth models.

Since most tumor types do not have predictable growth patterns, clinical implementation of the method would focus on providing a visual interpretation of future involvement regions of the tumor, under the assumption that it continues its trends from the past. This additional source of visual information can be very helpful in determining a situation of stable disease and for the decision making process of patients who undergo a long-term and non-invasive treatment.

Universally accepted gold standards for the validation of future predicted scan have not been developed yet. To provide an error measure for our method, we conducted a study in which experienced radiologists blindly manually segmented the tumor regions in the current, predicted, and actual future scans. The study included four patients with Optic Path Gliomas (OPGs) and four with GBMs. The comparison between the tumors segmented volumes in the predicted scans vs the actual future scans yield a mean surface distance error of 0.4mm and 0.83mm, and a mean volume overlap difference of 13.65% and 34.23% for the OPG and GBM patients, respectively. To the best of our knowledge, this is the first method that estimates a future scan based on patient specific tumor growth trends in previous scans.

2 Method

The inputs to our method are $N + 1$ consecutive rigidly registered (with the method in [5]) T1-weighted contrast-enhanced pulse sequence MRIs of the same patient acquired at roughly equal time intervals, $I_t, I_{t-1}, \dots, I_{t-N}$. The output is the estimation of the next scan of the patient in the time series.

The method consists of two steps. In the first step, the optical flow over time for every voxel in the current scan is computed. In the second step, the future transformation fields are estimated with an autoregressive model for groups of voxels. Fig. 1 shows a representative slice from the past, current, predicted, and actual future scans.

2.1 Temporal Optical Flow Computation

In this step, we compute the spatial path of each voxel in the current scan over time. First, we find the non-rigid transformation field between every two consecutive scans of the patient. We use the method of Kroon et al. [6], itself adapted from [7], to MRI scans. For every pair of consecutive scans, the method computes three transformation fields, one for every axis. This results in N forward and backward transformation fields. The forward transformation fields are $\{\mathbf{F}_{t-i}(\bar{r})\}_{i=1}^N$, where $\mathbf{F}_{t-i}(\bar{r})$ is the 3-dimensional forward transformation field from scan I_{t-i} to scan I_{t-i+1} , and $\bar{r} = (x, y, z)$ represents the spatial location in the scan. Similarly, $\{\mathbf{B}_{t-i}(\bar{r})\}_{i=1}^N$ are the backward transformation fields.

Next, we define the motion matrix optical flow for the patient’s scans. The matrix $\tilde{\mathbf{V}}$ is a 5-dimensional matrix whose dimensions are *(scan dimensions)* $\times 3 \times N$, representing the 3D motions of every voxel in the scan over time. We define $\mathbf{V} = \tilde{\mathbf{V}}(\bar{r}, \cdot, \cdot)$ as a $3 \times N$ matrix, where $\mathbf{V}(\bar{r}, i)$ is a 3×1 vector representing the motion of the voxel in location \bar{r} from time $(t-i)$ to $(t-i+1)$. The elements of $\mathbf{V}(\bar{r}, i)$ are recursively computed by:

$$\mathbf{V}(\bar{r}, i) = F_{t-i}(\bar{r}_{t-i+1} + B_{t-i}(\bar{r}_{t-i+1})) \quad (1)$$

where

$$\bar{r}_{t-i+1} = \begin{cases} \bar{r} & \text{when } i = 1 \\ \bar{r}_{t-i+2} + B_{t-i+1}(\bar{r}_{t-i+2}) & \text{otherwise} \end{cases} \quad (2)$$

and \bar{r} is the location of the voxel in the latest scan, I_t . $\mathbf{V}(\bar{r}, \cdot)$ is the spatial path over time of a voxel from the baseline scan I_{t-N} to the current scan I_t .

2.2 Estimation of Future Transformation Field

Next, we estimate the future motion of a voxel based on its past motions. To have sufficient statistical predictive power, we estimate the model parameters for every group of voxels assuming that voxels with similar past motion values follow the same prediction model. For this, we cluster all the voxels in the image into groups based on their past spatial flow.

We use the K-means clustering algorithm to group the voxels in the scan spatial space into K clusters based on their spatial flow over time, \mathbf{V} . We obtain K groups of voxels, where C_k is the number of voxels in the k -th group.

To predict the future scan of the patient, we estimate $\mathbf{V}(\bar{r}, t)$, i.e. we predict the future motion optical flow for each voxel. For every voxels cluster, we model the future motion as a linear combination of past motions, expressed by an autoregressive (AR) model:

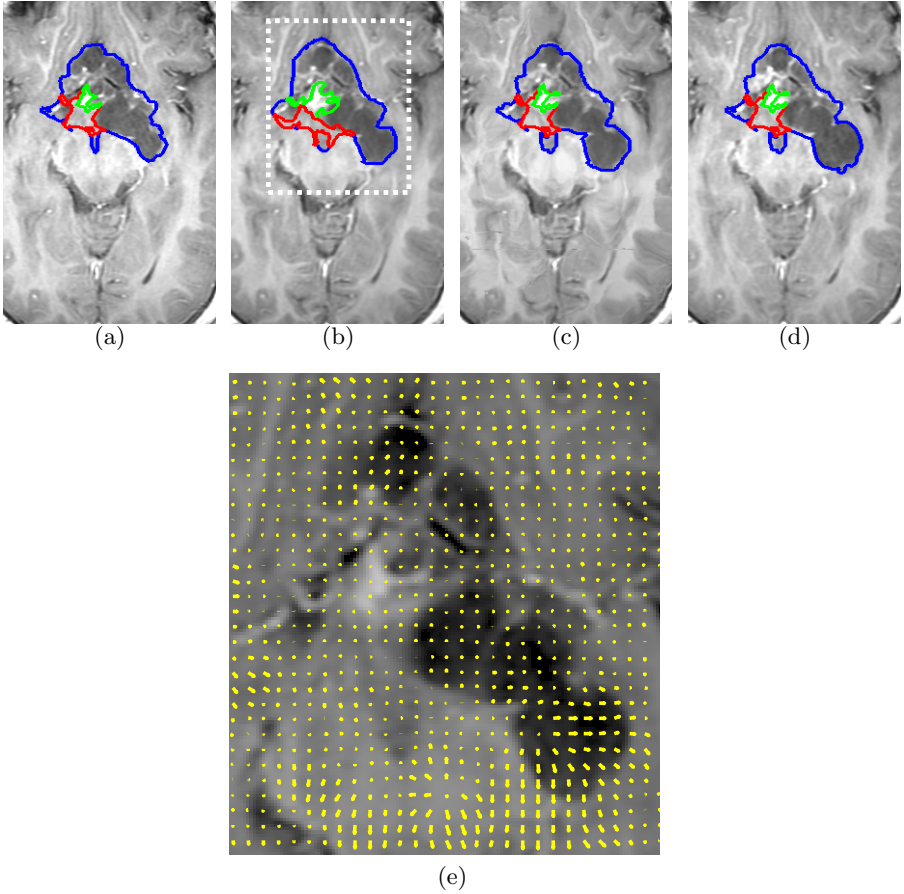


Fig. 1. Illustration of our method on a representative slice of T1-weighted pulse sequence of an OPG tumor and its internal components: (a) past scan; (b) current scan; (c) predicted scan; (d) actual acquired future scan – the tumor components are solid (red), enhancing (green) and cyst (blue), and; (e) estimated future transformation field projected on the scan plane and overlaid on the dashed area of the current scan – the yellow arrows indicate the local direction of the estimated future transformation field. Observe in the bottom right region of the image in (e) that the algorithm successfully predicted the expansion of the cyst component of the tumor.

$$\bar{v}_l(i) = \sum_{j=1}^p \mathbf{A}_k(j) \cdot \bar{v}_l(i-j) \quad (3)$$

where $\bar{v}_l(i)$ denotes the 3D optical flow motions from time $(t-i)$ to $(t-i+1)$ of a voxel in the k -th group, and p is the model order, $p \leq N$. Note that k is the index over clusters and l is the index of voxels in the cluster. The 3×3 matrices $\mathbf{A}_k(j)$ include the AR coefficients of the process, each corresponding to a specific lag, for the k -th cluster. This model describes a Multiple-Input-Multiple-Output (MIMO)

system, where the same prediction coefficients are used for all the voxels in the k -th group. Minimizing the forward prediction error in the least squares sense for this model, we obtain the Yule-Walker equations [8] of the MIMO model:

$$\sum_{j=1}^p \mathbf{A}_k(j) \mathbf{R}_v(i-j) = \mathbf{R}_v(i) \quad 1 \leq i \leq p \quad (4)$$

Note that, unlike the traditional MIMO case where $\mathbf{R}_v(n)$ is the autocorrelation of a multivariate process at lag n , here $\mathbf{R}_v(n)$ is the spatial mean of the temporal autocorrelation functions of the v_l at lag n , i.e.:

$$\mathbf{R}_v(n) = E_l(E_i[(\bar{v}_l(i)) \cdot (\bar{v}_l(i+n))]) \quad (5)$$

Assuming that $(v_1(n), v_2(n), \dots, v_{C_k}(n))$ are independent, identically distributed (i.d.d) with zero mean for every n , the sample covariance is:

$$\hat{\mathbf{R}}_v(n) = \frac{1}{C_k} \sum_{l=1}^{C_k} \frac{1}{N-n} \sum_{j=1}^{N-n} \bar{v}_l(j) \cdot \bar{v}_l(n+j)^T \quad (6)$$

Substituting (6) in (4) yields a set of linear equations which are solved with the Levinson-Durbin recursion [8].

The result is an estimation for the forward transformation field, $\mathbf{F}_t(\bar{r}) = \mathbf{V}(\bar{r}, t)$. Figs. 1(e) and 2(e) show examples of these fields. Finally, this transformation field is applied to the current image, I_t to obtain the estimation of the next future scan in the time series, I_{t+1} .

3 Experimental Results

We conducted a retrospective quantitative evaluation of our method with clinical gadolinium enhanced T1-weighted MRI scan series of eight patients. Patients did not undergo surgical interventions during the period of the research. Patients were divided into two groups. The first group consisted of four Neurofibromatosis (NF) patients, 3-7 years old subjects with OPGs which were scanned at approximately 6-month intervals. The second groups consisted of four adult GBM patients which were scanned at approximately 2-month intervals. All scans were acquired by a General Electric Signa 1.5T HDXT scanner. Each scan has $512 \times 512 \times 90$ voxels with isotropic voxel size of $1mm^3$.

Every patient was scanned five times at different time points. The first four scans were used to predict the fifth scan with our method. Based on empirical tests, we set the model order p to 3. We tested the method's performance for different values of K in the range 50-500 and we obtained the optimal results for our datasets at $K=100$. An expert radiologists manually produced tumor segmentations for the current, predicted, and the actual future scans using Analyze Direct 7.0 (Mayo Clinic, Rochester, MN).

Figs. 1 and 2 show representative results of the method. Table 1 shows the volume overlap error (VOE) and the mean surface distance (SD) of the manually

segmented tumor volumes in the predicted scans vs. the actual future scans. Detailed explanation about our validation measures can be found in [9]. For comparison, the same validation metrics were also computed for the segmented tumors in the current scan vs. the actual future scan. It can be seen that the method provides better results on GBM than OPG. This phenomenon can be explained by the fact the GBM is an aggressive tumor, that changes much more rapidly than OPG.

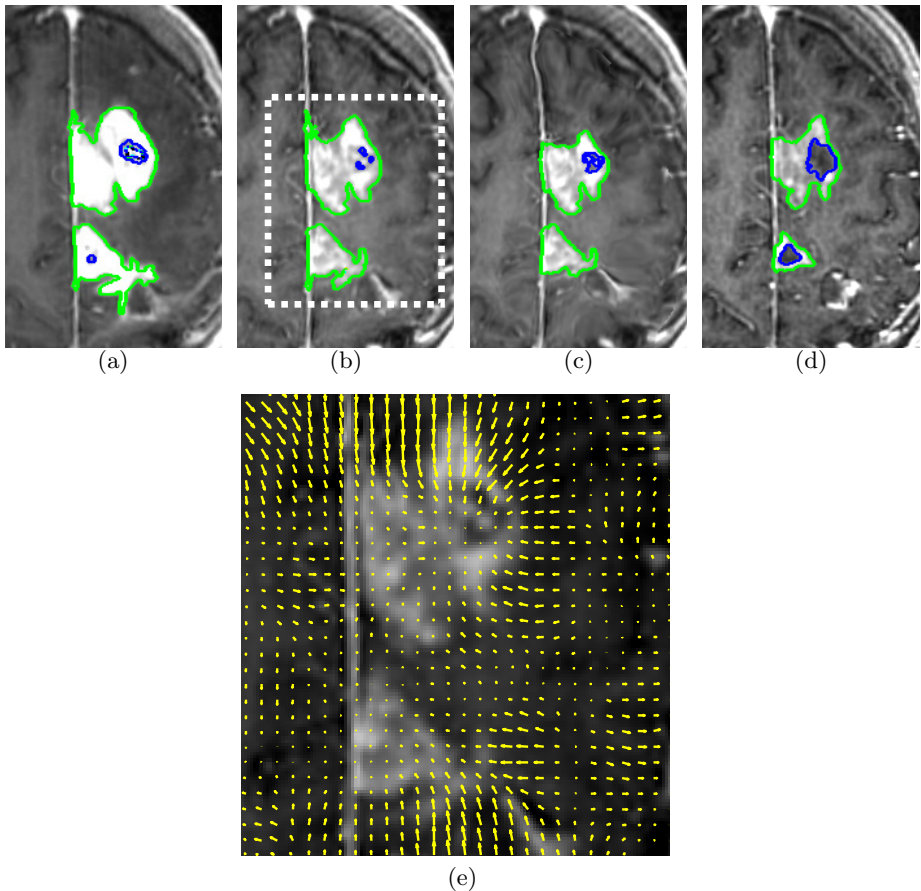


Fig. 2. Illustration of the method on a representative slice of T1-weighted pulse sequence of an GBM tumor and its internal components: (a) past scan; (b) current scan; (c) predicted scan; (d) actual acquired future scan – the components are: enhancing (green) and necrotic (blue); (e) estimated future transformation field projected on the scan plane and overlaid on the dashed area of the current scan – the yellow arrows indicate the local direction of the estimated future transformation field. Note how the algorithm successfully predicted the regression of the enhancing part of the tumor and the enlargement of the necrotic area.

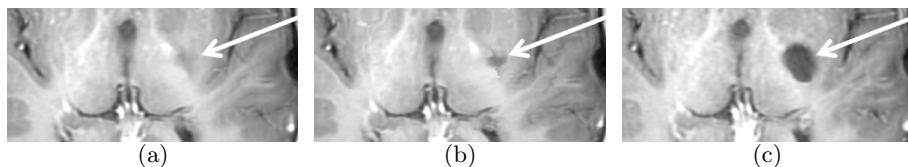


Fig. 3. A representative slice of T1-weighted pulse sequence from (a) current scan; (b) predicted scan, and; (c) actual acquired future scan. The arrow points to a new region of involvement of the tumor. Note that the new area of involvement is clearly noticeable in the predicted scan, although it is barely seen in the current scan.

Table 1. Volumetric overlap and mean surface distance of manual segmentation results: Current and predicted scans vs. actual future scan. The p-values were computed with the Wilcoxon signed rank test.

		Volumetric overlap error [%]		Mean surface distance [mm]	
	Patient #	Predicted vs. Actual future	Current vs. Actual future	Predicted vs. Actual future	Current vs. Actual future
OPG patients	1	32.9	32.8	1.21	1.15
	2	9.4	13.1	0.13	0.2
	3	8.3	23.3	0.22	0.75
	4	4	5.8	0.03	0.05
Average (OPG)		13.65	18.75	0.4	2.15
p-value (OPG)		0.25		0.375	
GBM patients	5	21.2	84.7	0.73	51.88
	6	25.1	65.1	0.18	1.47
	7	54.3	65.3	1.35	1.68
	8	36.3	38.5	1.038	1.29
Average (GBM)		34.23	63.4	0.83	14
p-value (GBM)		0.125		0.125	

We conclude from Table 1 that the VOE between the predicted segmented tumor vs. the actual future tumor is in many cases substantially lower than the one between the current and actual future ones. This indicates that when the method successfully estimated the future growing trend of the tumor, the predicted scan is more similar to the actual future scan than the current scan is.

A key new feature of our method is its ability to expand and emphasize new regions of tumor involvement during their early stage, in which they can be easily missed by the radiologist. Consider for example Fig. 3, which shows a representative slice from the current, predicted, and actual future scans. Note that while the infiltration of the cystic component into the slice can hardly be noticed in the current scan, this trend is emphasized in the predicted scan. This provides a clear early indication for this future involvement area of the tumor.

4 Conclusions

We have presented a new method for the estimation of patient’s future MR scan based on his/her past scans based on an auto-regression model of the voxel’s

optical flow over time. Since our method does not rely on a tumor-specific growth model, it can be used for a wide variety of tumor types. Experimental results on two types of brain tumors, OPG and GBM, show the successful prediction of the tumor growth, in terms of volumetric tumor overlap with the segmentation of the actual future scan.

A key advantage of our method is that it is fully automatic and that it does not require any user intervention for tumor localization. Furthermore, it predicts a whole scan rather than a specific tumor region of interest. Therefore, it has the potential to emphasize, in the predicted scan, tumor regions in their initial stage, that can hardly be noticed in the current scan.

Our method has several limitations. First, it cannot handle a surgical intervention performed between scans, as the prediction based on scans before the surgery most likely will hamper the prediction process. Second, the autoregressive assumption might not hold for all cases. In these cases, a specific tumor growth model has to be taken into account for a better prediction. Finally, the method would fail to predict substantial changes in tumor growth, which have no evidence in the past, or cases where the future trend of tumor growth is opposite to the one seen in the past.

The potential clinical significance of the brain tumor prediction is to provide the clinicians with a better picture of the tumor growth trends. The predicted scan can then be used to detect future involvement area of the tumor and to assist the decision-making process. Our future work will include the generalization of the method to include other MR sequences in the prediction process. In addition, we will examine the methods' performance on other types of tumors.

References

1. Hogeia, C., Davatzikos, C., Biros, G.: Modeling Glioma Growth and Mass Effect in 3D MR Images of the Brain. In: Ayache, N., Ourselin, S., Maeder, A. (eds.) MICCAI 2007, Part I. LNCS, vol. 4791, pp. 642–650. Springer, Heidelberg (2007)
2. Clatz, O., Sermesant, M., Bondiau, P.Y., Delingette, H., Warfield, S., Malandain, G., Ayache, N.: Realistic simulation of the 3D growth of brain tumors in MR images coupling diffusion with biomechanical deformation. *IEEE Transactions on Medical Imaging* 24(10), 1334–1346 (2005)
3. Mardor, Y., Roth, Y., Ocherashvilli, A., Spiegelmann, R., Tichler, T., Daniels, D., Maier, S.E., Nissim, O., Ram, Z., Baram, J., Orenstein, A., Pfeffer, R.: Pretreatment prediction of brain tumors' response to radiation therapy using high b-value diffusion-weighted MRI. *Neoplasia* 6(2), 136–142 (2004)
4. Lancaster, J.A., Carrington, B.M., Sykes, J.R., Jones, A.P., Todd, S.M., Cooper, R., Buckley, D.L., Davidson, S.E., Logue, J.P., Hunter, R.D., West, C.M.: Prediction of radiotherapy outcome using dynamic contrast enhanced MRI of carcinoma of the cervix. *International Journal of Radiation Oncology Biology Physics* 54(3), 159–767 (2002)
5. Friston, K.J., Holmes, A.P., Ashburner, J.: Statistical parametric mapping, SPM (1999), <http://www.fil.ion.ucl.ac.uk/spm/>
6. Kroon, D.J., Slump, C.: MRI modality transformation in demon registration. In: *IEEE International Symposium on Biomedical Imaging: From Nano to Macro*, pp. 963–966 (2009)

7. Thirion, J.: Image matching as a diffusion process: an analogy with maxwells demons. *Medical Image Analysis* 2(3), 243–260 (1998)
8. Morettin, P.A.: The Levinson algorithm and its applications in time series analysis. *International Statistical Review / Revue Internationale de Statistique* 52(1), 83–92 (1984)
9. Gerig, G., Jomier, M., Chakos, M.: Valmet: A New Validation Tool for Assessing and Improving 3D Object Segmentation. In: Niessen, W., Viergever, M. (eds.) *MICCAI 2001*. LNCS, vol. 2208, pp. 516–523. Springer, Heidelberg (2001)